High beta-cell mass prevents streptozotocin-induced diabetes in thioredoxin-interacting protein-deficient mice

Elodie A.Y. Masson, Shlomit Koren, Fathima Razik, Howard Goldberg, Edwin P. Kwan, Laura Sheu, Herbert Y. Gaisano, George I. Fantus

Am J Physiol Endocrinol Metab 296: E1251–E1261, 2009.
First published February 17, 2009; doi:10.1152/ajpendo.90619.2008.

High β-cell mass prevents streptozotocin-induced diabetes in thioredoxin-interacting protein-deficient mice

Elodie Masson, Shlomit Koren, Fathima Razik, Howard Goldberg, Edwin P. Kwan, Laura Sheu, Herbert Y. Gaisano, and I. George Fantus

Department of Medicine, Mount Sinai Hospital, Toronto General Research Institute, Banting and Best Diabetes Centre, University Health Network and Department of Physiology, University of Toronto, Toronto, Ontario, Canada

Submitted 9 July 2008; accepted in final form 10 February 2009

Masson E, Koren S, Razik F, Goldberg H, Kwan EP, Sheu L, Gaisano HY, Fantus IG. High β-cell mass prevents streptozotocin-induced diabetes in thioredoxin-interacting protein-deficient mice. *Am J Physiol Endocrinol Metab* 296: E1251–E1261, 2009. First published February 17, 2009; doi:10.1152/ajpendo.90619.2008.—Thioredoxin-interacting protein (TxNIP) is an endogenous inhibitor of thioredoxin, a ubiquitous thiol oxidoreductase, that regulates cellular redox status. Diabetic mice exhibit increased expression of TxNIP in pancreatic islets, and recent studies suggest that TxNIP is a proapoptotic factor in β-cells that may contribute to the development of diabetes. Here, we examined the role of TxNIP deficiency in vivo in the development of insulin-deficient diabetes and whether it impacted on pancreatic β-cell mass and/or insulin secretion. TxNIP-deficient (Hcb-19/TxNIP$^{-/-}$) mice had lower baseline glycemia, higher circulating insulin concentrations, and higher total pancreatic insulin content and β-cell mass than control mice (C3H). Hcb-19/TxNIP$^{-/-}$ did not develop hyperglycemia when injected with standard multiple low doses of streptozotocin (STZ), in contrast to C3H controls. Surprisingly, although β-cell mass remained higher in Hcb-19/TxNIP$^{-/-}$ mice compared with C3H after STZ exposure, the relative decrease induced by STZ was as great or even greater in the TxNIP-deficient animals. Consistently, cultured pancreatic INS-1 cells transfected with small-interfering RNA against TxNIP were more sensitive to cell death induced by direct exposure to STZ or to the combination of inflammatory cytokines interleukin-1β, interferon-γ, and tumor necrosis factor-α. Furthermore, when corrected for insulin content, isolated pancreatic islets from TxNIP$^{-/-}$ mice exhibited reduced glucose-induced insulin secretion. These data indicate that TxNIP functions as a regulator of β-cell mass and influences insulin secretion. In conclusion, the relative resistance of TxNIP-deficient mice to STZ-induced diabetes appears to be because of an increase in β-cell mass. However, TxNIP deficiency is associated with sensitization to STZ- and cytokine-induced β-cell death, indicating complex regulatory roles of TxNIP under different physiological and pathological conditions.

thioredoxin interacting protein; pancreatic β-cell; apoptosis; insulin secretion

DIABETES IS ASSOCIATED WITH AN INABILITY of the pancreatic β-cells to meet insulin requirements and maintain normal metabolism, leading to hyperglycemia. In type 1 diabetes, β-cells are the specific target of an autoimmune assault, with an invasion of the islets by macrophages and T cells, termed insulitis. These activated inflammatory cells produce cytokines, such as interleukin-1β (IL-1β), interferon-γ (IFNγ), and tumor necrosis factor-α (TNF-α), which cause progressive destruction of most β-cells via apoptosis, leading to an absolute deficiency of insulin. At the time of diagnosis, β-cell mass is generally reduced by 70–80% (10, 13). Type 2 diabetes, on the other hand, is caused by a combination of insulin resistance and β-cell dysfunction, with impaired glucose-induced insulin secretion. The loss of glucose stimulation, characteristic of subjects with type 2 diabetes, is manifested by a lack of first-phase insulin release as well as decreased second phase secretion. However, the contribution of a loss of β-cell mass in the pathogenesis of the disease has recently been recognized, and there is evidence that apoptosis is also the main mode of β-cell death in type 2 diabetes (4, 10, 11, 26, 37). Considering that β-cell death might underlie both forms of diabetes, elucidation of the molecular processes associated with β-cell apoptosis and maintenance of β-cell mass are critical to develop new therapeutic strategies to prevent and/or delay these pathological events.

Thioredoxin-interacting protein (TxNIP), also known as thioredoxin-binding protein 2 or vitamin D_3-upregulated protein 1, is an endogenous inhibitor of the ubiquitous thiol oxidoreductase, thioredoxin. As a result, TxNIP promotes oxidative stress (28, 31) and has also been found to enhance apoptosis and inhibit cell growth in a variety of cell types (6, 14, 22, 27, 33, 34). The expression of the TxNIP gene and protein is increased in several tissues of diabetic animal models, including pancreatic islets of *ob*/*ob* and nonobese insulin-resistant AZIP-F_1 transgenic mice (22). In vitro, the TxNIP gene is strongly upregulated by high glucose concentrations. In particular, TxNIP expression has been reported to be dramatically increased in pancreatic β-cells, as well as human and murine pancreatic islets exposed to high glucose (22, 29). Furthermore, recent in vitro data support the concept that TxNIP is a proapoptotic factor and a potential mediator of glucotoxicity in β-cells. Thus Minn et al. (22) demonstrated that overexpression of TxNIP promoted apoptosis in the INS-1 rat β-cell line. Subsequently, the same group reported that Exendin 4, an agonist of glucagon-like peptide-1 receptor, suppressed TxNIP expression, and that TxNIP overexpression blunted the anti-apoptotic effects of Exendin 4 in INS-1 cells treated with H_2O_2 (6). In addition, high glucose-induced apoptosis in isolated islets from wild-type mice was associated with increased TxNIP protein levels, whereas isolated islets from TxNIP-deficient (Hcb-19) mice displayed resistance to high-glucose-stimulated apoptosis (8).

The goal of this study was to examine the role of TxNIP deficiency in the development of insulin-deficient diabetes in vivo and whether any effect involved β-cell survival and/or insulin secretion. We investigated the Hcb-19 mouse strain, a congenic strain variant of C3H mice, which carries a nonsense mutation in the TxNIP gene leading to a dramatic decrease in

Address for reprint requests and other correspondence: I. G. Fantus, Dept. of Medicine, Mount Sinai Hospital, 60 Murray St., Lebovic Bldg, Rm. 5028, Toronto, ON, Canada M5T 3L9 (e-mail: gfantus@mtsinai.on.ca).

TxNIP expression (2). Streptozotocin (STZ), an agent toxic to β-cells, was used to induce a well-characterized immune-mediated model of insulin-deficient diabetes mellitus. We found that, in contrast to control mice, Hcb-19/TxNIP$^{-/-}$ mice did not develop hyperglycemia in response to the standard, multiple low-dose STZ administration protocol. This "resistance" to STZ appeared to result from a higher basal insulin reserve (plasma insulin concentrations, total pancreatic insulin content, and β-cell mass) rather than from a protection against β-cell death. Indeed, isolated islets from Hcb-19/TxNIP$^{-/-}$ mice showed no protection against STZ or cytokine-induced apoptosis compared with C3H controls, and RNAi-mediated TxNIP-deficient INS-1 β-cells in vitro were more sensitive to cell death induced by STZ or cytokines. At the same time, it was noted that glucose-induced insulin secretion was impaired in pancreatic islets isolated from Hcb-19/TxNIP$^{-/-}$ mice. These data support the notion that TxNIP deficiency plays a protective role in the development of diabetes by promoting the constitution of a higher initial β-cell mass, while at the same time it appears to sensitize β-cells to injury characteristic of type 1 diabetes. The latter findings, along with the apparent insulin secretory dysfunction, demonstrate the complex regulatory roles of TxNIP and its potential contribution to the development of diabetes mellitus.

MATERIALS AND METHODS

Animal Experiments

Hcb-19 and control C3H/DiSnA mice (generous gift of Dr. R. A. Davis, San Diego State University) were maintained under standardized conditions at the University Health Network animal facility (Toronto, Canada) and fed and provided water ad libitum. All procedures and experiments were approved by the University Health Network Animal Care Committee and carried out in accordance with the guidelines of the Canadian Council on Animal Care. The multiple low-dose STZ protocol recommended by the Animal Models of Diabetes Complications Consortium (http://www.amdcc.org/) was used to induce diabetes in 8-wk-old C3H and Hcb-19 male mice. STZ (in 0.1 M sodium citrate buffer, pH 4.5) (Sigma-Aldrich, St. Louis, MO) was injected intraperitoneally after a 6-h fast, at a dose of 50 mg/kg of body wt daily for five consecutive days. Control animals received the same volume per body weight of citrate buffer. Later (6 wk), a group of STZ-treated C3H and Hcb-19 mice received a second set of five STZ injections ("STZ 2×50" group). The experimental endpoint was reached 6 wk after STZ injections for the control and "STZ 50" groups and 2 wk after the second set of STZ injections for the STZ 2×50 group. Six hour fasting glycemia was monitored weekly throughout the experimental period via the tail vein using a glucometer (One Touch Ultra; Life Scan, Milpitas, CA). At the endpoint of the study, blood samples were collected on 6-h-fasted mice in EDTA tubes and centrifuged at 5,000 *g* for 5 min at 4°C. Plasma was collected and frozen at −80°C. Mice were subsequently euthanized with CO_2, and pancreases were removed and weighed. A small piece from the pancreatic tail was collected, weighed, and snap-frozen for measurement of total insulin content. The rest of the pancreas was cut into multiple pieces, fixed in 10% formalin for 24 h, and embedded in paraffin for histological analyses.

Measurement of Plasma Insulin Levels and Total Pancreatic Insulin Content

The piece of pancreas tail, or alternatively the entire pancreas, was homogenized in acid-ethanol (0.2 mmol/l HCl in 75% ethanol) to extract insulin. Insulin concentration of the pancreatic extract as well as plasma insulin levels were measured by enzyme-linked immunosorbent assay (ELISA), using a rat insulin kit (Linco Research, St. Charles, MO). Total pancreatic insulin content was calculated from the insulin concentration in the extracts corrected for total pancreas weights.

Immunohistochemistry

To estimate β-cell mass, two pancreatic sections from each mouse (200 μm apart) were stained for insulin using a 1:200 dilution of rabbit antibody (Biomeda, Plovdiv, Bulgaria) for 1 h after pepsin antigen retrieval and counterstained with hematoxylin. Slides were then digitalized using a brightfield scanner (ScanScope XT; Aperio Technologies, Vista, CA). The proportion of the pancreas occupied by the β-cells (relative β-cell area) was determined by distinguishing stained tissue (β-cells) from unstained (non β-cell area) using image analysis software (Aperio Image Scope; Aperio Technologies). β-Cell mass was calculated by multiplying the relative β-cell area by the wet weight of the pancreas as described (3). To detect apoptosis, TdT-dUTP nick end-labeling (TUNEL) and cleaved caspase-3 staining of two pancreas sections per mouse were performed. To detect proliferation, two sections per mouse were stained for Ki-67. Bromodeoxyuridine (BrdU) staining was performed on pancreas sections from mice administered 50 mg/kg body wt BrdU by intraperitoneal injection, 6 h before death. Analysis of serial consecutive sections stained with either one of the four markers cited above or insulin enabled identification of apoptotic or proliferative cells as insulin-immunopositive β-cells. The number of TUNEL, cleaved caspase-3, Ki-67, or BrdU-positive β-cells was determined per 100 islets.

Islet Isolation, Perifusion Secretory Assays, and Measurement of Apoptosis

Pancreatic islets were isolated as previously described (18). Briefly, a collagenase solution was injected in the common bile duct, and the pancreas was collected and digested by incubation at 37°C. Islets were handpicked in the pancreatic lysate and maintained overnight in 11

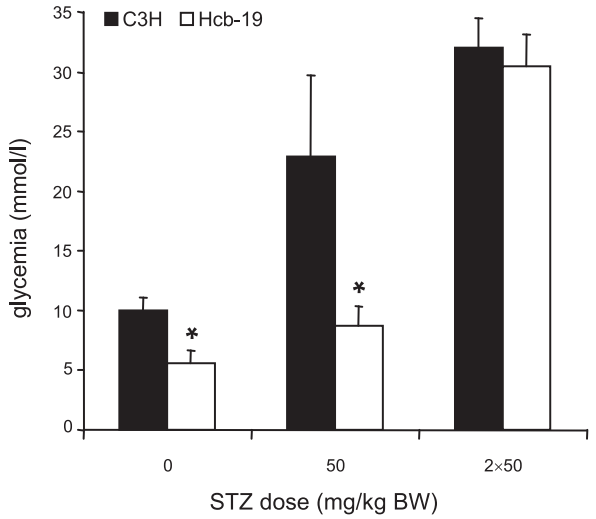

Fig. 1. Thioredoxin-interacting protein-deficient (Hcb-19/TxNIP$^{-/-}$) mice do not develop hyperglycemia in response to the low-dose streptozotocin (STZ) protocol. Control mice (C3H) and Hcb-19/TxNIP$^{-/-}$ mice were injected ip with either citrate buffer or 50 mg/kg of body wt STZ daily for 5 consecutive days. The "2 × 50" groups received a second set of 5 STZ injections 6 wk later. Fasting glucose (6 h) levels were measured via the tail vein using a glucometer 6 wk after STZ injections for the control and "50" groups and 2 wk after the second set of injections for the 2 × 50 groups. Results are expressed as means ± SD, 4 independent experiments (n = 18–28 mice) for the control and 50 groups and 2 independent experiments (n = 8 mice) for the 2 × 50 groups. *$P < 0.05$ vs. C3H.

mM glucose RPMI 1640, supplemented with 10% FBS and penicillin/streptomycin. Batches of 50–60 islets were placed in a perifusion chamber (capacity 1.3 ml) at 37°C and perifused at a flow rate of ~1 ml/min with a Krebs-Ringer bicarbonate buffer (KRB). Islets were first equilibrated for 30 min in KRB HEPES buffer supplemented with 2.8 mmol/l glucose. They were then stimulated with 16.7 mmol/l glucose for a 30-min period. Fractions were collected at different time points for insulin determination using a radioimmunoassay (Linco Research). At the end of the perifusion, islets were collected and lysed in acidic ethanol for measurement of insulin content. Results are presented as insulin secreted normalized per islet and per total insulin content. Alternatively, after the overnight recovery period, batches of 50 islets were placed in 5 mM glucose RPMI medium and treated with a combination of the proinflammatory cytokines IL-1β (2 ng/ml), IFNγ (100 ng/ml), and TNF-α (10 ng/ml) (R & D Systems, Minneapolis, MN) for 48 h, 3 days, or 5 days or with 1 or 2 mM STZ for 24 h. At the end of the treatment periods, islets were lysed, and apoptosis was assessed by determination of mono- and oligonucleosomes using an enzyme immunoassay (Cell Death Detection ELISAPLUS; Roche Diagnostics, Mannheim, Germany) according to the manufacturer's instructions.

Cell Culture

INS-1 832/13 cells (rat pancreatic β-cell line originally described in Ref. 1) were maintained in RPMI 1640 medium (11.1 mM glucose, 1 mM sodium pyruvate, and 10 mM HEPES) (GIBCO-Invitrogen, Carlsbad, CA) supplemented with 10% FBS, 2 mM L-glutamine, 55 μM β-mercaptoethanol, and penicillin/streptomycin at 37°C and 5% CO_2. For the experiments, INS-1 cells cultured in 5 mM glucose medium were exposed to 25 mM glucose for 24 h, or 0.1, 0.5, or 1 mM STZ for 1 h, followed by a 6-h recovery period. Alternatively, cells were treated with a combination of 1 ng/ml IL-1β, 50 ng/ml IFNγ, and 5 ng/ml TNF-α for 24 h to 3 days. At the end of the

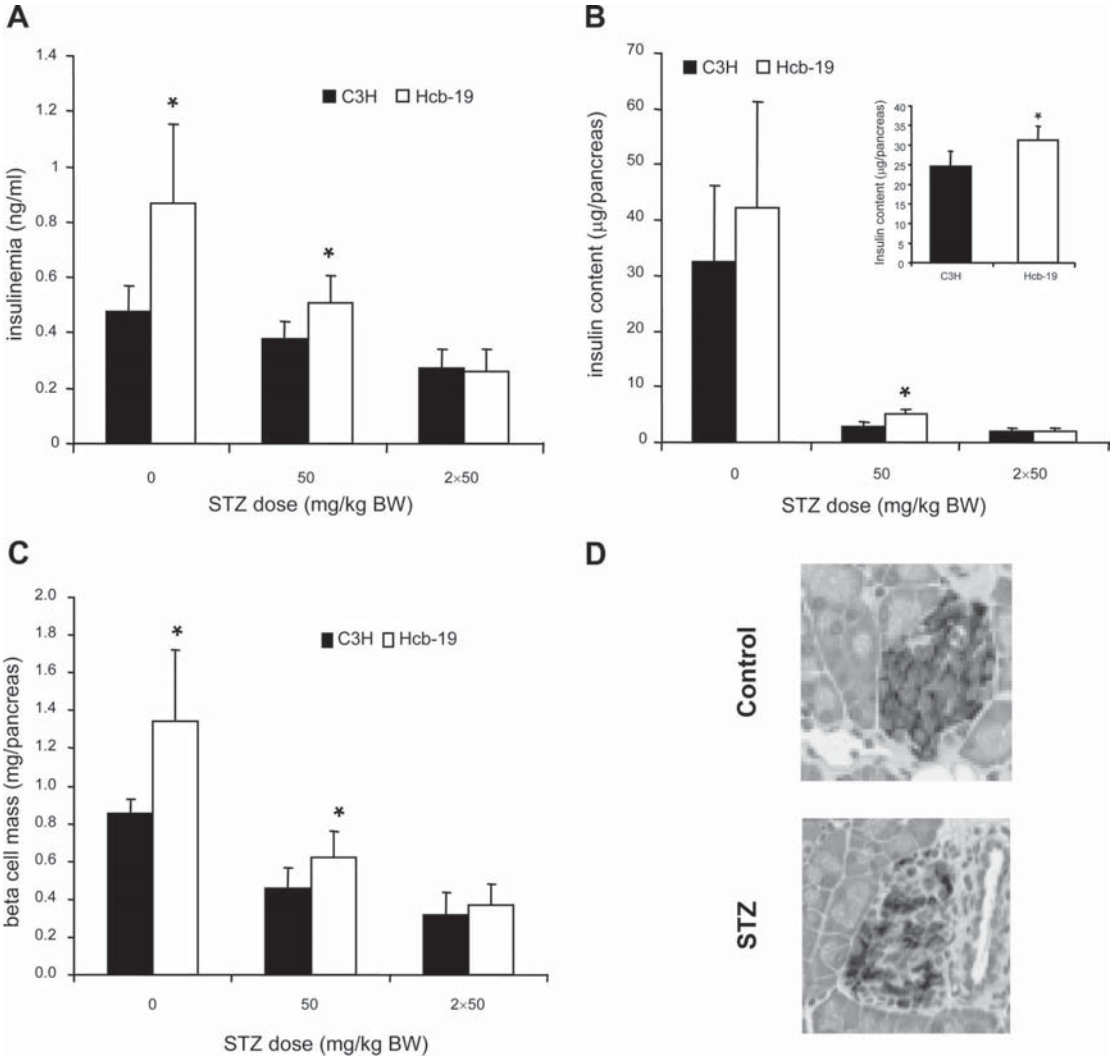

Fig. 2. Hcb-19/TxNIP$^{-/-}$ mice have higher insulin levels, total pancreatic insulin content, and β-cell mass than C3H mice. C3H and Hcb-19/TxNIP$^{-/-}$ mice were injected ip with either citrate buffer or 50 mg/kg of body wt STZ daily for 5 consecutive days. The 2 × 50 groups received a second set of 5 STZ injections 6 wk later. *A*: blood samples were collected on 6-h-fasted mice at 6 wk after STZ injections for the control and 50 groups and at 2 wk after the second set of injections for the 2 × 50 groups. Plasma was used to measure insulin levels by enzyme-linked immunosorbent assay (ELISA; $n = 5–8$). *B*: a small piece of the pancreas tail was used to determine the total insulin content by ELISA after acidic ethanol extraction as described in MATERIALS AND METHODS ($n = 7–13$). Total insulin content was also measured on extracts of the entire pancreas of mice under control conditions (inset; $n = 7$). *C*: pancreas was fixed, and 2 sections from each mouse were stained for insulin to assess β-cell mass, using automated image analysis software ($n = 5–9$). Bars represent means ± SD. *$P < 0.05$ vs. C3H group. *D*: representative photomicrographs.

treatment times indicated, the cell culture supernatant was collected, and floating and attached cells were washed with PBS and lysed in RIPA buffer containing protease inhibitors for 30 min on ice. Cell lysates were centrifuged at 16,000 *g* for 10 min at 4°C. The supernatant was used to determine protein concentration using the Bradford assay (Bio-Rad Laboratories, Hercules, CA) and analyzed by Western blotting. For RNA interference experiments, INS-1 cells were forward transfected with small-interfering RNA (siRNA) control or directed against TxNIP (Stealth RNAi; Invitrogen) using Lipofectamine RNAimax, according to the manufacturer's instructions (Invitrogen). As a preliminary experiment, three different sequences at increasing concentrations (1, 5, and 10 nM) were tested for their efficiency to decrease TxNIP expression by Western Blotting in INS-1 cells 3 days after transfection. One of them was selected and used at the lowest efficient dose of 1 nM. Transfected cells were then exposed to cytokines or STZ as described above. Attached cells were collected using Trypsin and pooled with the floating cells contained in the culture medium, washed, and stained with annexin V and propidium iodide using a cell death kit according to the manufacturer's instructions (Calbiochem, EMD Chemicals, Merck, Darmstadt, Germany). Apoptosis and necrosis were studied by flow cytometry using a BD FACS Aria cell sorter (BD Biosciences, San Jose, CA). Results were analyzed using FlowJo software (Tree Star, Ashland, OR).

Western Blotting

Protein lysates were separated by SDS-PAGE and transferred to nitrocellulose membranes. The membranes were blocked using PBS-0.05% Tween 20 with 5% nonfat milk for 1 h, then incubated overnight at 4°C with the indicated primary antibody. Protein bands were detected with secondary antibodies conjugated to horseradish peroxidase (Santa Cruz Biotechnology, Santa Cruz, CA) and an enhanced chemiluminescence system (LumiGlo; Mandel, Guelph, ON, Canada). The following primary antibodies were used: mouse TxNIP (1:1,000 dilution; MBL, Woburn, MA) and rabbit β-tubulin (1:1,500 dilution; Santa Cruz Biotechnology).

Statistical Analyses

Results are given as means ± SD. Statistical significance was assessed by two-tailed unpaired *t*-test. $P < 0.05$ was considered to be significant.

RESULTS

Hcb-19/TxNIP$^{-/-}$ Mice do not Develop Diabetes in Response to Low-Dose STZ Administration

The multiple low-dose STZ administration protocol has been widely used in rodents to induce insulin-deficient diabetes similar to type 1 diabetes while minimizing generalized non-specific toxic effects of this chemical agent (19, 23, 35). TxNIP$^{-/-}$ (Hcb-19) and wild-type control (C3H) mice received five consecutive daily intraperitoneal injections of STZ at a dose of 50 mg/kg body wt. Controls for both groups were injected with citrate, the STZ vehicle. As shown in Fig. 1, and in agreement with previously published data (7, 12, 16, 30), Hcb-19/TxNIP$^{-/-}$ mice had lower glucose levels than C3H control mice under basal conditions, i.e., in the absence of STZ exposure (5.6 ± 1.0 vs. 10 ± 1.1 mmol/l for Hcb-19 and C3H, respectively, $P < 0.05$). Interestingly, Hcb-19/TxNIP$^{-/-}$ mice did not develop hyperglycemia while the C3H control mice were overtly diabetic 6 wk after STZ injections (STZ 50 groups: 8.7 ± 1.6 vs. 22.9 ± 6.8 mmol/l for Hcb-19 and C3H, respectively, $P < 0.05$). All C3H mice developed diabetes to varying degrees in response to one set of five STZ injections. Only 4 out of 26 Hcb-19 mice exhibited hyperglycemia under these conditions. A second set of five STZ injections was required in the mutant mice to induce high blood glucose levels similar to those measured in the C3H control strain (STZ 2×50 groups, Fig. 1). These observations indicate that Hcb-19/TxNIP$^{-/-}$ mice are "resistant" to STZ-induced diabetes.

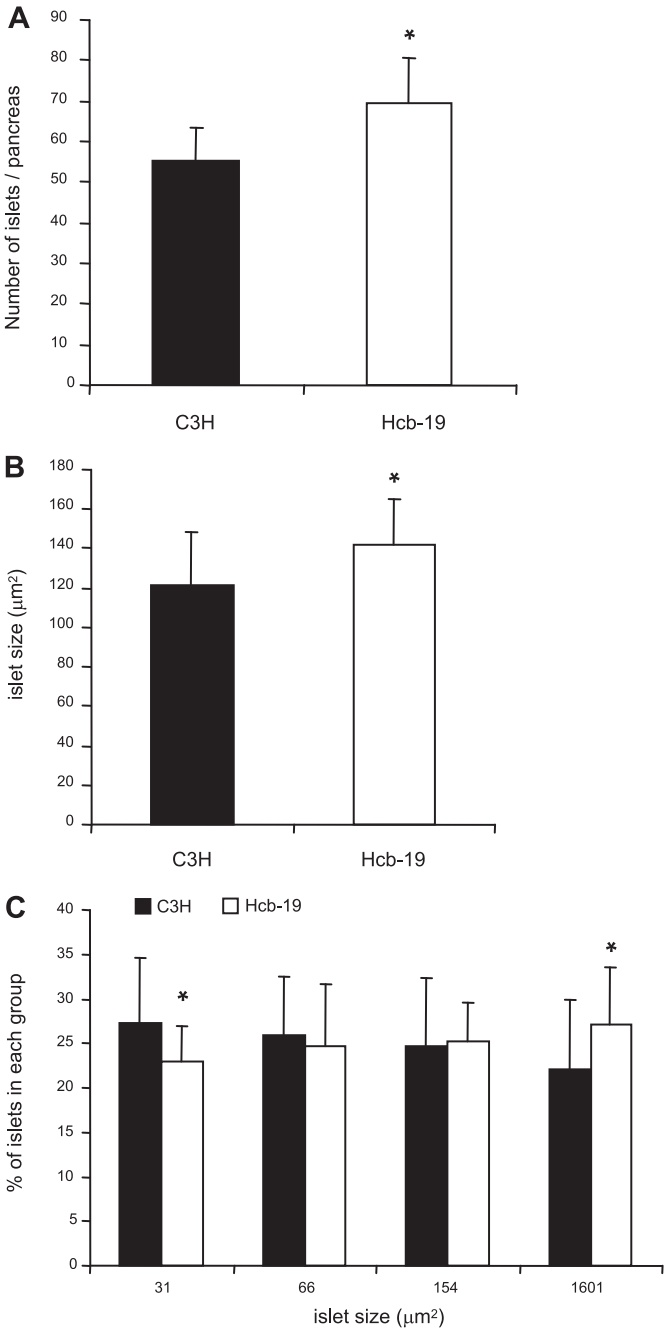

Fig. 3. Hcb-19/TxNIP$^{-/-}$ mice have more and larger pancreatic islets than C3H mice. Pancreas of C3H and Hcb-19/TxNIP$^{-/-}$ mice were fixed, sectioned, and stained for insulin. Islets (1,101) from 10 C3H mice and islets (1,245) from 9 Hcb-19 mice were counted and sized. The no. of islets/pancreas section (*A*) and the average size of individual islets (*B*) are shown, as well as the quartile distribution of islet size (*C*). *Quartile 1* = 15–31; *quartile 2* = 31–66; *quartile 3* = 66–154; and *quartile 4* = 154–1,601 μm^2. Results are expressed as means ± SD. *$P < 0.05$ vs. C3H group.

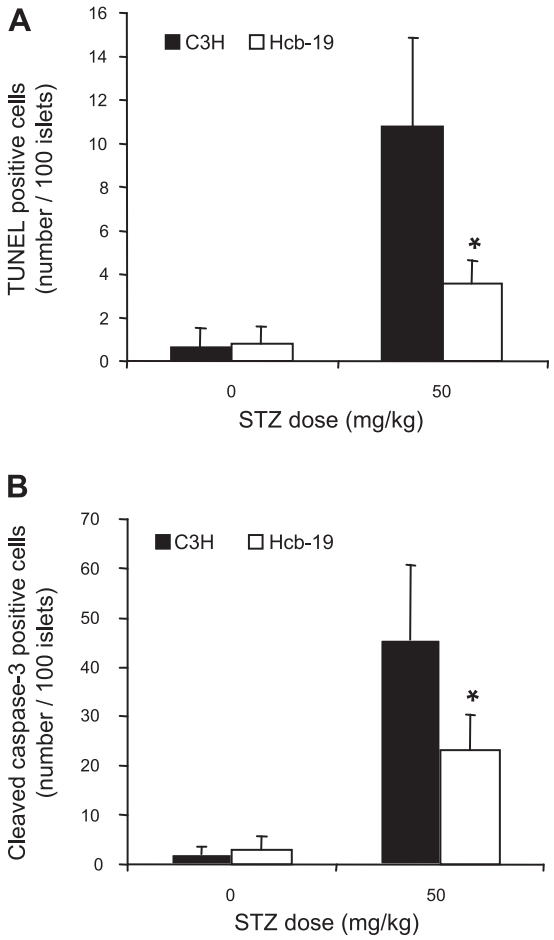

Fig. 4. Apoptosis of β-cells 1 day after the last of 5 STZ injections. C3H and Hcb-19/TxNIP$^{-/-}$ mice received 5 consecutive daily injections of 50 mg/kg body wt STZ or citrate buffer and were euthanized 1 day later. Pancreas was collected and fixed, and serial sections were stained for TdT-dUTP nick end-labeling (TUNEL) or cleaved caspase-3 to detect apoptosis and for insulin to localize the positive cells to insulin-immunopositive β-cells. The number of β-cells positive for TUNEL (*A*) and cleaved caspase-3 (*B*) staining/100 islets is shown. Results are expressed as means ± SD (n = 5–8). *$P < 0.05$ vs. C3H group.

Hcb-19/TxNIP$^{-/-}$ Mice Have a Greater Insulin Reserve Than C3H Controls

We next assessed some of the potential causes of the relative resistance to diabetes exhibited by the Hcb-19/TxNIP$^{-/-}$ mice. At the experimental endpoint, plasma was collected after a 6-h fast to measure insulin levels. In addition, pancreatic tissue was harvested to determine total insulin content and β-cell mass by immunohistochemistry. Under basal conditions, in the absence of STZ administration, Hcb-19/TxNIP$^{-/-}$ mice exhibited a 1.8-fold higher circulating insulin concentration (Fig. 2*A*), a 1.3-fold higher pancreatic insulin content (Fig. 2*B*), and a 1.6-fold higher β-cell mass (Fig. 2*C*) compared with C3H mice. More detailed analyses of pancreas sections showed a small but significant increase in islet number per pancreas, as well as a higher average size of individual islets (Fig. 3, *A* and *B*). There was also a higher proportion of larger islets in the Hcb-19/TxNIP$^{-/-}$ mice that appeared to account for the higher β-cell mass (Fig. 3*C*). There was no difference in terms of islet β-cell density (number of β-cells/individual islet area) or individual β-cell size (data not shown). As shown in Fig. 2*D*, photomicrographs of pancreatic sections stained for insulin depict well-delineated islets with an abundance of insulin stored in the β-cells.

STZ treatment leads to distortion of islet architecture with loss of insulin-producing β-cells and degranulation of surviving β-cells. Surprisingly, the relative reduction of insulin reserve following STZ exposure appeared to be at least as large or even greater in Hcb-19/ TxNIP$^{-/-}$ mice than in C3H controls. Thus circulating insulin levels were decreased by 21 and 41%, whereas β-cell mass was reduced by 45 and 54% in C3H and Hcb-19/ TxNIP$^{-/-}$ mice, respectively, suggesting that a larger proportion of β-cells were actually destroyed by STZ in TxNIP-deficient mice. Despite this apparently greater damage induced by STZ, circulating insulin, total pancreatic insulin content, and β-cell mass remained significantly higher in Hcb-19/ TxNIP$^{-/-}$ mice than in C3H after the first set of STZ injections (STZ 50 groups). Only after the repeated injections (STZ 2 × 50 groups) were these parameters similar between the two strains (Fig. 2, *A–C*), and at that point, correlated with the similar degree of hyperglycemia (Fig. 1). These data suggested that the "resistance" to STZ of the Hcb-19/TxNIP$^{-/-}$ mice was due, at least in part, to the higher baseline insulin reserve, manifested by higher β-cell mass and pancreatic insulin content.

Assessment of Apoptosis in Hcb-19/TxNIP$^{-/-}$ β-Cells In Vivo and Ex Vivo

Because changes in β-cell mass are dependent on the balance between the rate of β-cell death and proliferation (or neogenesis), we investigated whether the STZ effect on β-cell apoptosis and proliferation was different between the two strains.

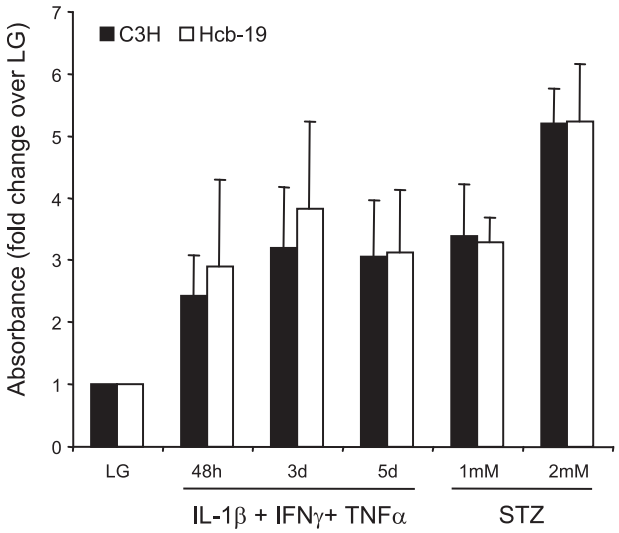

Fig. 5. STZ and inflammatory cytokines induce similar degrees of apoptosis in pancreatic islets isolated from Hcb-19/TxNIP$^{-/-}$ and C3H mice. Pancreatic islets were isolated from C3H and Hcb-19/TxNIP$^{-/-}$ mice, and batches of 50 islets were treated with a combination of interleukin (IL)-1β, interferon (IFN)-γ, and tumor necrosis factor (TNF)-α for increasing periods of time (0–5 days), or with 1 or 2 mM STZ for 24 h, as described in MATERIALS AND METHODS. At the end of the treatment periods, apoptosis was assessed by determination of mono- and oligonucleosomes using an enzyme immunoassay. Results are expressed as means ± SD (n = 3–6).

In vivo studies. Pancreatic tissue was collected 1 day after the last STZ injection, and serial sections were stained for insulin, TUNEL assay, or cleaved caspase-3. Only rare apoptotic β-cells were detected in histological sections from control pancreas tissue (mice injected with vehicle alone). The number of both TUNEL and caspase-3 positive β-cells was markedly increased in sections from STZ-treated mice (Fig. 4). However, the overall percentage of apoptotic cells detected in pancreas sections of STZ-treated mice appeared to be relatively few considering the marked decrease in β-cell mass observed. This may have been a consequence of the fact that this measure of apoptosis provides only a single snapshot of a dynamic process and that dead cells are quickly cleared in vivo by macrophages. The number of apoptotic β-cells detected in Hcb-19/TxNIP$^{-/-}$ pancreatic sections was significantly lower, 33 and 50% of that observed in C3H mice as assessed by TUNEL (Fig. 4*A*) and cleaved caspase-3 staining (Fig. 4*B*), respectively. In addition, pancreatic tissue collected 1 day and 2 wk after the last STZ injection was stained for insulin and Ki-67 or BrdU to evaluate proliferation. Although an increase in the proportion of proliferative β-cells in response to STZ was observed 2 wk after the last STZ injection, in contrast to apoptosis, there were no differences between the two strains in these markers of proliferation (data not shown). Although these data suggest that Hcb-19/TxNIP$^{-/-}$ mouse β-cells may be less sensitive to STZ-induced apoptosis than those in the C3H wild type, this conclusion would be inconsistent with the fact that the relative reduction in β-cell mass in response to STZ exposure was greater in Hcb-19/TxNIP$^{-/-}$ mice (Fig. 2*C*).

Ex vivo studies. To investigate this phenomenon further, we performed ex vivo measurements of apoptosis in pancreatic islets isolated from C3H control and Hcb-19/TxNIP$^{-/-}$ mice. In STZ-injected mice, β-cell death results from both an initial, direct cytotoxic effect of STZ and a subsequent immune reaction mediated by inflammatory cytokines IL-1β, IFNγ, and TNF-α (23). Therefore, isolated islets were treated directly with STZ or with a combination of these three cytokines for different time periods. Apoptosis was then assessed by determination of mono- and oligonucleosome levels. Results presented in Fig. 5 show that every treatment tested induced a significant degree of apoptosis in pancreatic islets. The induction ranged from ~2.5 (48 h cytokine treatment)- to 5 (2 mM STZ)-fold. However, we observed no statistically significant differences in apoptosis levels between the two strains of mice under any of these conditions. Of note, basal levels of apoptosis (without any treatment) were slightly higher in Hcb-19/TxNIP$^{-/-}$ islets compared with C3H controls [arbitrary units: 0.220 ± 0.097 vs. 0.191 ± 0.069, P = not significant (NS)]. These ex vivo data do not support the notion that TxNIP deficiency provides resistance against β-cell apoptosis induced by STZ or inflammatory cytokines.

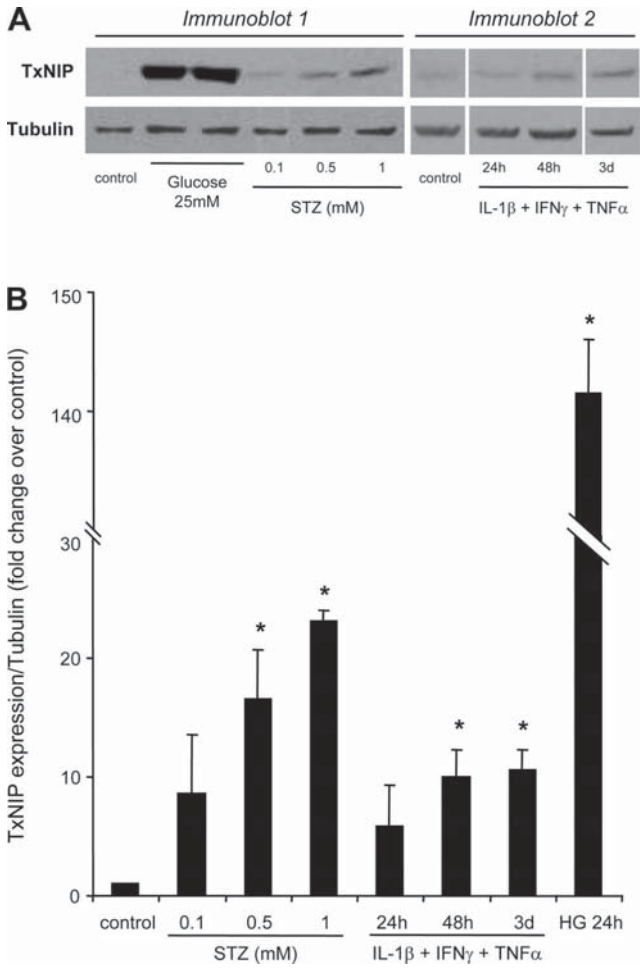

Fig. 6. Treatment with high glucose, STZ, or the combination of IL-1β, IFNγ, and TNF-α induces TxNIP protein expression in INS-1 cells. INS-1 cells were cultured in 5 mM glucose medium (control) or exposed to various treatments (25 mM glucose for 24 h and 0.1, 0.5, or 1 mM STZ for 1 h), followed by a 6-h recovery period or a combination of 1 ng/ml IL-1β, 50 ng/ml IFNγ, and 5 ng/ml TNF-α for 24 h, 48 h, or 3 days. Protein lysates were analyzed by immunoblotting for TxNIP and β-tubulin, to verify equal loading, as described in MATERIALS AND METHODS. *A*: representative immunoblots of 3 independent experiments. In *immunoblot A2*, the bands at the 24- and 48-h time points were separated from the original image to be displayed in chronological sequence. *B*: results are expressed as means ± SD of fold changes vs. control (no treatment). *$P < 0.05$ vs. control group.

Effects of STZ and Inflammatory Cytokines in Cultured INS-1 cells: Role of TxNIP

To determine whether TxNIP expression was affected by STZ and/or proinflammatory cytokines, cultured INS-1 β-cells were treated with increasing concentrations of STZ for 1 h followed by 6 h recovery or with a combination of IL-1β, IFNγ, and TNF-α for 24 h to 3 days. Cells were also exposed

Fig. 7. TxNIP-deficient INS-1 cells are more sensitive to STZ and cytokine-induced cell death than control cells. INS-1 cells were transfected with 1 nM small-interfering RNA (siRNA), control (scrambled), or directed against TxNIP, in 5 mM glucose RPMI medium, and exposed to either a combination of 1 ng/ml IL-1β, 50 ng/ml IFNγ, and 5 ng/ml TNF-α for the indicated times, or to STZ for 1 h followed by a 6-h recovery period at the indicated concentrations. Floating and attached cells were then collected. *A*: TxNIP expression was determined by Western blotting. Bands shown were obtained from a single gel in which replicate bands were removed. Alternatively, cells were stained for annexin V and propidium iodide (PI) before analysis by flow cytometry. *B* and *C*: representative FACS plots with average percentages in each quadrant (*B*) and percentage of nonviable cells (*C*). AnV−, PI−: viable cells; AnV+, PI−: early apoptotic cells; AnV+, PI+: late apoptotic/necrotic cells; AnV−, PI+: necrotic cells. Results are expressed as means ± SD (n = 4–7). *$P < 0.05$ vs. siRNA control (CTR).

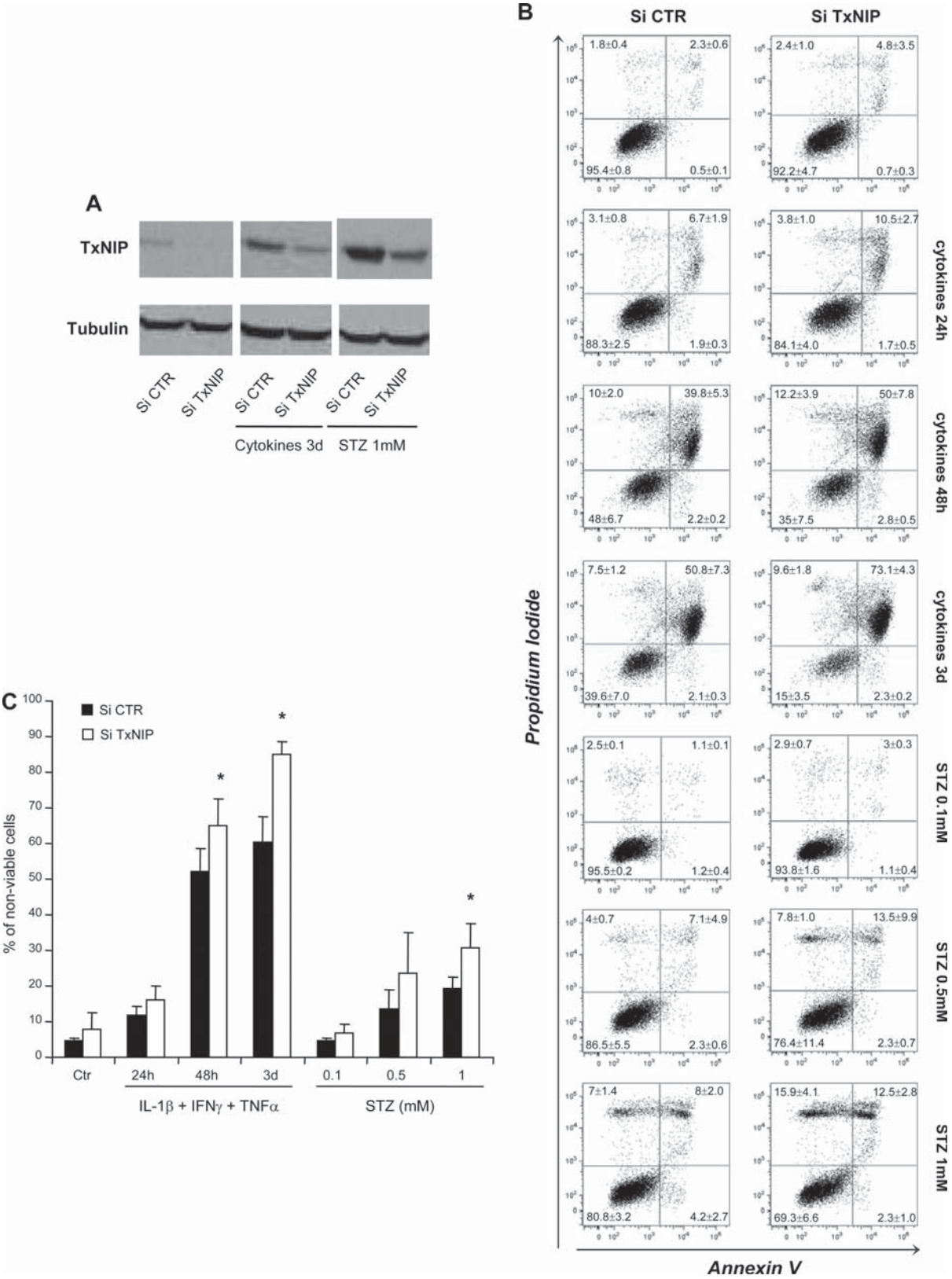
A
TxNIP
Tubulin
Si CTR
Si TxNIP
Si CTR
Si TxNIP
Si CTR
Si TxNIP
Cytokines 3d
STZ 1mM
B
Si CTR
Si TxNIP
1.8±0.4
2.3±0.6
95.4±0.8
0.5±0.1
2.4±1.0
4.8±3.5
92.2±4.7
0.7±0.3
3.1±0.8
6.7±1.9
88.3±2.5
1.9±0.3
3.8±1.0
10.5±2.7
84.1±4.0
1.7±0.5
cytokines 24h
10±2.0
39.8±5.3
48±6.7
2.2±0.2
12.2±3.9
50±7.8
35±7.5
2.8±0.5
cytokines 48h
7.5±1.2
50.8±7.3
39.6±7.0
2.1±0.3
9.6±1.8
73.1±4.3
15±3.5
2.3±0.2
cytokines 3d
2.5±0.1
1.1±0.1
95.5±0.2
1.2±0.4
2.9±0.7
3±0.3
93.8±1.6
1.1±0.4
STZ 0.1mM
4±0.7
7.1±4.9
86.5±5.5
2.3±0.6
7.8±1.0
13.5±9.9
76.4±11.4
2.3±0.7
STZ 0.5mM
7±1.4
8±2.0
80.8±3.2
4.2±2.7
15.9±4.1
12.5±2.8
69.3±6.6
2.3±1.0
STZ 1mM
Propidium Iodide
Annexin V
C
Si CTR
Si TxNIP
% of non-viable cells
Ctr
24h
48h
3d
0.1
0.5
1
IL-1β + IFNγ + TNFα
STZ (mM)

to high glucose concentrations (25 mM), as a positive control (8, 22). Western blot analyses showed that both STZ and cytokine exposure significantly induced TxNIP protein expression, although to a lesser extent than high glucose, with a maximum induction of 23- and 11-fold for STZ and cytokine treatment, respectively, vs. 142-fold for high glucose (Fig. 6).

We next aimed to investigate the significance of the STZ- and cytokine-induced increase in TxNIP expression in cultured β-cells and determine the role that TxNIP deficiency might play in pancreatic β-cell death. To this end, TxNIP expression was downregulated in INS-1 cells using RNA interference. As shown in Fig. 7*A*, TxNIP siRNA was able to efficiently decrease TxNIP protein expression and inhibit its induction by STZ and cytokine treatment. INS-1 cells transfected with control (scrambled) or TxNIP siRNA were then exposed, as described above, to various concentrations of STZ or a combination of IL-1β, IFNγ, and TNF-α for the times indicated, and cell death was investigated by flow cytometry using annexin V and propidium iodide as markers of apoptosis and necrosis, respectively. As expected, the different treatments caused a significant amount of cell death, increasing with duration and concentration (Fig. 7*B*). Although cytokine exposure led mainly to a marked augmentation of the annexin V-positive, propidium iodide-positive cell population (late apoptotic cells), STZ treatment resulted in an additional significant increase of highly propidium iodide-positive (necrotic) cells. Of particular interest, the results indicated that the proportion of dying/dead cells was greater in TxNIP-deficient compared with control cells under every treatment condition (Fig. 7*C*). It should be noted that, in the case of STZ, this was not accounted for by the increased necrosis, since the apoptotic cell populations were also elevated (Fig. 7*B*). These data are consistent with the in vivo observation of STZ-induced loss of β-cell mass and indicate that TxNIP-deficient cells are more sensitive to STZ- and cytokine-induced cell death. We noted that the basal level of cell death in TxNIP siRNA transfected cells, in the absence of any treatment, appeared to be slightly higher (P = NS) than that seen in control siRNA transfected cells. While we cannot exclude nonspecific effects of RNA interference, this observation suggests that abnormally low levels of TxNIP may impair INS-1 pancreatic β-cell viability.

Hcb-19/TxNIP$^{-/-}$ Pancreatic Islets Manifest Decreased Glucose-Induced Insulin Secretion

The hyperinsulinemia combined with lower glycemia observed in the present study, as well as in previous reports (7, 16, 30), may be interpreted as indicative of a greater insulin secretory capacity of Hcb-19/TxNIP$^{-/-}$ islets. This question has not been specifically investigated in previous studies. To examine this directly, pancreatic islets were isolated from Hcb-19/TxNIP$^{-/-}$ and C3H control mice and perifused. Batches of 50 to 60 islets were stimulated with glucose to determine the insulin secretory capacity of individual islets ex vivo. First, the results showed that Hcb-19/TxNIP$^{-/-}$ islets had a higher insulin content than C3H controls (48 ± 15.6 vs. 30 ± 8.6 ng/islet for Hcb-19 and C3H, respectively, $P < 0.05$) (Fig. 8*A*). Second, mutant Hcb-19 islets exhibited a small decrease in glucose-induced insulin secretion when corrected for islet number (P = NS; Fig. 8, *B* and *C*). However, when the data were normalized for total insulin content, glucose-induced secretion was markedly reduced in Hcb-19/TxNIP$^{-/-}$ islets (area under the curve = 4.2 ± 3.4 vs. 10.9 ± 5.5 pg·min·ml^{-1}·ng^{-1} for Hcb-19 and C3H, respectively, $P < 0.05$; Fig. 8, *D* and *E*). Of note, both the initial peak (first phase) and the subsequent sustained insulin secretion (second phase) were affected. It should also be noted that basal insulin secretion was similar when corrected for islet insulin content. These data strongly suggest that the higher circulating insulin levels exhibited by Hcb-19/TxNIP$^{-/-}$ mice are due to the greater islet cell mass, rather than increased β-cell secretory capacity. Combined with increased peripheral glucose uptake, and/or impaired hepatic glucose production, this would contribute to the lower glycemia observed in this strain.

DISCUSSION

The biological functions of TxNIP are not completely defined. Based on its binding and inhibitory action on thioredoxin, it has been suggested to regulate cellular redox state and promote oxidative stress (28, 31). In various cell types, TxNIP has been found to inhibit proliferation and/or promote apoptosis (6, 14, 22, 27, 33, 34). The observation that TxNIP gene expression is markedly upregulated by glucose has led to investigation of its role in glucose metabolism and the pathophysiological effects of hyperglycemia. The availability of TxNIP-deficient mouse models has proven valuable to obtain further insight into the biological roles of TxNIP in vivo. In the present study, we used the Hcb-19/ TxNIP$^{-/-}$ mouse model, which harbors a TxNIP gene nonsense mutation, and showed that these mice exhibit a higher insulin reserve (circulating insulin levels, total pancreatic insulin content, and β-cell mass) in the basal state compared with strain-matched C3H controls. TxNIP deficiency was associated with a relative resistance to STZ-induced diabetes mellitus. Thus, whereas C3H controls developed marked hyperglycemia after receiving the standard five injections of the low-dose STZ protocol, the TxNIP-deficient mice remained normoglycemic. A second set of STZ injections was required to induce significant hyperglycemia. After this second set and concomitant with the rise in circulating glucose concentrations, circulating insulin levels, pancreatic insulin content, and β-cell mass were decreased to similar levels in the Hcb-19/TxNIP$^{-/-}$ animals as in the C3H wild type. These observations are consistent with the recent study of Chen et al. (7), reported while this work was underway. Indeed, the authors observed similar findings of higher β-cell mass and resistance against STZ-induced diabetes in the Hcb-19/TxNIP$^{-/-}$ mouse model, as well as in a β-cell specific TxNIP knockout, confirming that the observed resistance is a pancreatic effect and not the consequence of the unique metabolic phenotype of the Hcb-19 model (16). In addition, they showed that TxNIP deficiency protects the leptin-deficient *ob*/*ob* mouse from the development of type 2 diabetes.

Unexpectedly, we observed that the β-cell mass was more dramatically affected in Hcb-19/TxNIP$^{-/-}$ mice compared with C3H after STZ exposure. This strongly suggests that the normoglycemia and higher β-cell mass exhibited by TxNIP-deficient mice after the standard low-dose STZ protocol is the result of the higher initial β-cell mass and that TxNIP-deficient β-cells may be paradoxically more sensitive to STZ-induced cell death. However, this appeared to be in contradiction with the fact that fewer apoptotic β-cells were detected in pancreatic

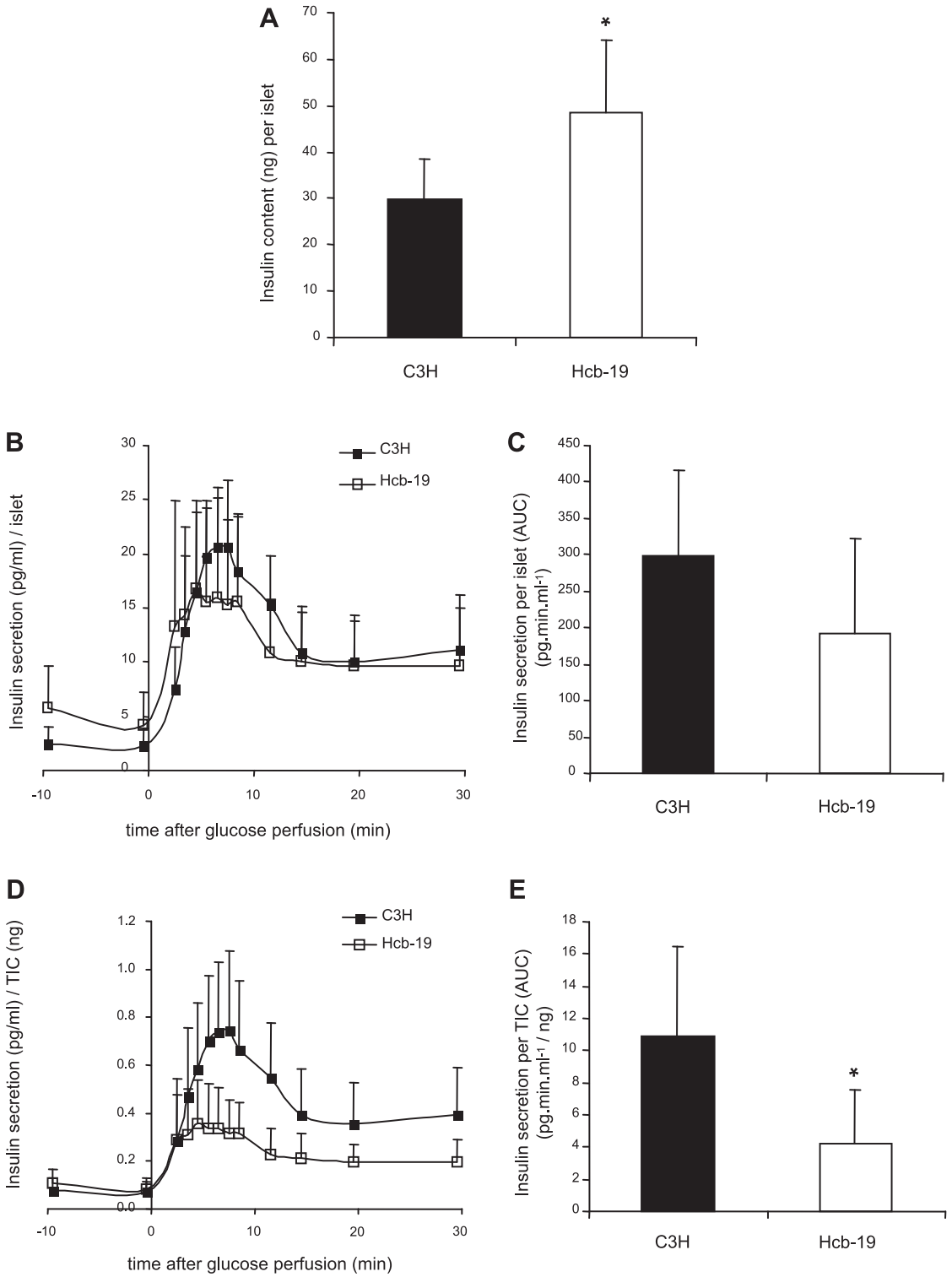

Fig. 8. Pancreatic islets of Hcb-19/TxNIP$^{-/-}$ mice have higher insulin content but lower glucose-induced insulin secretion than C3H islets. Pancreatic islets were isolated from C3H and Hcb-19/TxNIP$^{-/-}$ mice. Batches of 50–60 islets were perifused with a Krebs-Ringer bicarbonate buffer and then stimulated with 16.7 mmol/l glucose. Fractions were collected for insulin determination at different time points. *A*: at the end of the perifusion, islets were collected and lysed for measurement of insulin content by radioimmunoassay. *B* and *C*: insulin secretion/islet over 30 min (*B*) and area under the curve (AUC; *C*) calculated above basal per islet. *D* and *E*: insulin secretion normalized for total insulin content (TIC). Results are expressed as means ± SD ($n = 8$). *$P < 0.05$ vs. C3H group.

sections of Hcb-19/ TxNIP$^{-/-}$ mice compared with C3H after STZ injection. Furthermore, a reduction in β-cell apoptosis was reported to be associated with TxNIP deficiency in the β-cell-specific knockout model exposed to STZ, as well as in the *ob*/*ob* model (7). It is important to note that staining of pancreatic sections in these studies gave only a single time point or snapshot of the apoptotic process and that dead cells are completely and rapidly cleared in vivo. Thus the lower

number of detected apoptotic cells in the Hcb-19/TxNIP$^{-/-}$ mice observed in the present study 1 day after the last STZ injection does not prove that fewer cells actually died. The timing and/or rate of β-cell death and clearance may also be different between the two strains. For example, TxNIP-deficient β-cells could have undergone apoptosis before control cells and have already been cleared at the time of measurement. Of note, Chen et al. (7) did not quantify β-cell mass before and after STZ exposure. Therefore, although these investigators proposed that TxNIP deficiency enhanced β-cell mass and protected against β-cell apoptosis, whether overall fewer or more β-cells were destroyed by STZ exposure in their models was not documented.

A potentially greater sensitivity of TxNIP-deficient β-cells to STZ-induced cell death in vivo was consistent with our in vitro data obtained in INS-1 cells. In the context of STZ, it should be noted that there are similarities to the clinical and immunohistological features seen in human type 1 diabetes. Thus β-cell death results from both an initial, direct, cytotoxic effect (generation of free radicals and DNA strand breaks) and a subsequent immune reaction directed against the β-cell in response to tissue damage and protein modification (23, 35). Cytokine and chemokine expression by inflammatory cells, T cells, and macrophages is proposed to be the major pathogenetic mechanism leading to insulitis and β-cell apoptosis (15, 17, 19–21, 23, 35, 36). To link our in vivo observations to this proposed STZ-induced pathophysiology, we downregulated TxNIP expression in cultured INS-1 β-cells using SiRNA and exposed them to STZ or the cytokines IL-1β, IFNγ, and TNF-α. The results indicated that TxNIP$^{-/-}$ cells are more sensitive to STZ- and cytokine-induced death. Although TxNIP overexpression has been associated with cell death/apoptosis in various cell types (8, 14, 27, 33, 34), it appears that abnormally low levels of TxNIP expression might also be deleterious for cell survival. In addition, we observed that, although STZ and inflammatory cytokines induced a large amount of cell death in INS-1 cells, these agents increased TxNIP expression to a much lower extent than high glucose. Moreover, despite the blockade of increased TxNIP expression by RNA interference, STZ and cytokines still dramatically induced β-cell death. This suggests the possibility that STZ and/or cytokines on one hand, and high glucose on the other hand, might exert their effects on β-cell death via distinct mechanisms. Although TxNIP has been implicated in high glucose-induced β-cell apoptosis (8), it does not appear to be required for β-cell death in response to STZ or cytokines.

Finally, the effects of TxNIP on insulin secretion have not been extensively investigated. In the current study, we show that glucose-stimulated insulin secretion corrected for total insulin content of individual islets from Hcb-19/TxNIP$^{-/-}$ mice is reduced when compared with C3H wild-type mouse islets. The perifusion experiments suggest that TxNIP signaling might affect both the initial primed pool of insulin granules accounting for first phase release as well as the subsequent recruitment of granules that accounts for the second phase. In contrast, Chen et al. (8) reported that insulin secretion was unchanged in Hcb-19/TxNIP$^{-/-}$ islets. This discrepancy is likely due to the fact that, in the latter study, insulin secretion was expressed per islet and not corrected for islet insulin content, which was higher in the Hcb-19/TxNIP$^{-/-}$ mice. In fact, the higher circulating insulin levels we, and others (16, 30), observe in Hcb-19/TxNIP$^{-/-}$ mice is likely the result of the higher β-cell mass and total islet insulin content, which more than compensate for the impaired insulin secretory capacity of the β-cells.

Recently, TxNIP deficiency was found to be associated with increased protein kinase B (Akt) signaling. Thus Akt mRNA and protein levels, as well as phosphorylation, were increased in isolated islets of both Hcb-19/TxNIP$^{-/-}$ and β-cell-specific TxNIP knockout mice (7). Relevant to insulin secretion, the phenotype of transgenic mice overexpressing active Akt1 in β-cells has been shown to be similar to TxNIP-deficient mice; namely, they exhibit an increased islet mass, hyperinsulinemia, and a resistance to STZ-induced diabetes. However, they also demonstrate an impaired insulin secretion in response to glucose when corrected for β-cell mass (32). Together, these observations raise the possibility that TxNIP deficiency may impair insulin secretion of pancreatic islets by inducing Akt signaling.

In summary, the present data indicate that TxNIP is involved in the constitution of β-cell mass and that the greater β-cell mass observed in TxNIP$^{-/-}$ mice accounts for their resistance to STZ-induced diabetes. The development of islets and islet cell mass are determined, in part, during a neonatal remodeling period, when there is a high degree of β-cell replication and apoptosis (3). This may influence individual susceptibility to diabetes by limiting β-cell mass early in life (11). Considering the complex roles TxNIP appears to play in β-cell survival and function, further investigation is warranted to determine the involvement of TxNIP in islet cell development.

ACKNOWLEDGMENTS

We thank Dr. R. A. Davis, San Diego State University, for providing us with the C3H/Hcb-19 mouse model.

GRANTS

This work was supported by Grant Nos. MOP 38009 and MOP 49409 from the Canadian Institutes of Health Research to I. G. Fantus. E. Masson was supported by a Canadian Diabetes Association postdoctoral fellowship, an award from the Faculty of Medicine, and a Banting and Best Diabetes Centre postdoctoral fellowship, University of Toronto. F. Razik was supported by a Summer Studentship from the Samuel Lunenfeld Research Institute, Mount Sinai Hospital.

REFERENCES

1. **Asfari M, Janjic D, Meda P, Li G, Halban PA, Wollheim CB.** Establishment of 2-mercaptoethanol-dependent differentiated insulin-secreting cell lines. *Endocrinology* 130: 167–178, 1992.
2. **Bodnar JS, Chatterjee A, Castellani LW, Ross DA, Ohmen J, Cavalcoli J, Wu C, Dains KM, Catanese J, Chu M, Sheth SS, Charugundla K, Demant P, West DB, de Jong P, Lusis AJ.** Positional cloning of the combined hyperlipidemia gene Hyplip1. *Nat Genet* 30: 110–116, 2002.
3. **Bonner-Weir S.** beta-cell turnover: its assessment and implications. *Diabetes* 50, *Suppl* 1: S20–S24, 2001.
4. **Butler AE, Janson J, Bonner-Weir S, Ritzel R, Rizza RA, Butler PC.** Beta-cell deficit and increased beta-cell apoptosis in humans with type 2 diabetes. *Diabetes* 52: 102–110, 2003.
5. **Chen CL, Lin CF, Chang WT, Huang WC, Teng CF, Lin YS.** Ceramide induces p38 MAPK and JNK activation through a mechanism involving a thioredoxin-interacting protein-mediated pathway. *Blood* 111: 4365–4374, 2008.
6. **Chen J, Couto FM, Minn AH, Shalev A.** Exenatide inhibits beta-cell apoptosis by decreasing thioredoxin-interacting protein. *Biochem Biophys Res Commun* 346: 1067–1074, 2006.
7. **Chen J, Hui ST, Couto FM, Mungrue IN, Davis DB, Attie AD, Lusis AJ, Davis RA, Shalev A.** Thioredoxin-interacting protein deficiency

induces Akt/Bcl-xL signaling and pancreatic beta-cell mass and protects against diabetes. *FASEB J* 22: 3581–3594, 2008.
8. **Chen J, Saxena G, Mungrue IN, Lusis AJ, Shalev A.** Thioredoxin-interacting protein: a critical link between glucose toxicity and beta cell apoptosis. *Diabetes* 57: 938–944, 2008.
9. **Chutkow WA, Patwari P, Yoshioka J, Lee RT.** Txnip is a critical regulator of hepatic glucose production. *J Biol Chem* 283: 2397–2406, 2007.
10. **Cnop M, Welsh N, Jonas JC, Jorns A, Lenzen S, Eizirik DL.** Mechanisms of pancreatic beta-cell death in type 1 and type 2 diabetes: many differences, few similarities. *Diabetes* 54, *Suppl* 2: S97–S107, 2005.
11. **Donath MY, Halban PA.** Decreased beta-cell mass in diabetes: significance, mechanisms and therapeutic implications. *Diabetologia* 47: 581–589, 2004.
12. **Donnelly KL, Margosian MR, Sheth SS, Lusis AJ, Parks EJ.** Increased lipogenesis and fatty acid reesterification contribute to hepatic triacylglycerol stores in hyperlipidemic Txnip$^{-/-}$ mice. *J Nutr* 134: 1475–1480, 2004.
13. **Eizirik DL, Mandrup-Poulsen T.** A choice of death–the signal-transduction of immune-mediated beta-cell apoptosis. *Diabetologia* 44: 2115–2133, 2001.
14. **Han SH, Jeon JH, Ju HR, Jung U, Kim KY, Yoo HS, Lee YH, Song KS, Hwang HM, Na YS, Yang Y, Lee KN, Choi I.** VDUP1 upregulated by TGF-beta1 and 1,25-dihydorxyvitamin D3 inhibits tumor cell growth by blocking cell-cycle progression. *Oncogene* 22: 4035–4046, 2003.
15. **Holstad M, Sandler S.** A transcriptional inhibitor of TNF-alpha prevents diabetes induced by multiple low-dose streptozotocin injections in mice. *J Autoimmun* 16: 441–447, 2001.
16. **Hui TY, Sheth SS, Diffley JM, Potter DW, Lusis AJ, Attie AD, Davis RA.** Mice lacking thioredoxin-interacting protein provide evidence linking cellular redox state to appropriate response to nutritional signals. *J Biol Chem* 279: 24387–24393, 2004.
17. **Kolb-Bachofen V, Epstein S, Kiesel U, Kolb H.** Low-dose streptozocin-induced diabetes in mice. Electron microscopy reveals single-cell insulitis before diabetes onset. *Diabetes* 37: 21–27, 1988.
18. **Kwan EP, Xie L, Sheu L, Nolan CJ, Prentki M, Betz A, Brose N, Gaisano HY.** Munc13–1 deficiency reduces insulin secretion and causes abnormal glucose tolerance. *Diabetes* 55: 1421–1429, 2006.
19. **Like AA, Rossini AA.** Streptozotocin-induced pancreatic insulitis: new model of diabetes mellitus. *Science* 193: 415–417, 1976.
20. **Lukic ML, Stosic-Grujicic S, Shahin A.** Effector mechanisms in low-dose streptozotocin-induced diabetes. *Dev Immunol* 6: 119–128, 1998.
21. **Martin AP, Alexander-Brett JM, Canasto-Chibuque C, Garin A, Bromberg JS, Fremont DH, Lira SA.** The chemokine binding protein M3 prevents diabetes induced by multiple low doses of streptozotocin. *J Immunol* 178: 4623–4631, 2007.
22. **Minn AH, Hafele C, Shalev A.** Thioredoxin-interacting protein is stimulated by glucose through a carbohydrate response element and induces beta-cell apoptosis. *Endocrinology* 146: 2397–2405, 2005.
23. **O'Brien BA, Harmon BV, Cameron DP, Allan DJ.** Beta-cell apoptosis is responsible for the development of IDDM in the multiple low-dose streptozotocin model. *J Pathol* 178: 176–181, 1996.
24. **Oka S, Masutani H, Liu W, Horita H, Wang D, Kizaka-Kondoh S, Yodoi J.** Thioredoxin-binding protein-2-like inducible membrane protein is a novel vitamin D3 and peroxisome proliferator-activated receptor (PPAR)gamma ligand target protein that regulates PPARgamma signaling. *Endocrinology* 147: 733–743, 2006.
25. **Parikh H, Carlsson E, Chutkow WA, Johansson LE, Storgaard H, Poulsen P, Saxena R, Ladd C, Schulze PC, Mazzini MJ, Jensen CB, Krook A, Björnholm M, Tornqvist H, Zierath JR, Ridderstråle M, Altshuler D, Lee RT, Vaag A, Groop LC, Mootha VK.** TXNIP regulates peripheral glucose metabolism in humans. *PLoS Med* 4: el58, 2007.
26. **Sakuraba H, Mizukami H, Yagihashi N, Wada R, Hanyu C, Yagihashi S.** Reduced beta-cell mass and expression of oxidative stress-related DNA damage in the islet of Japanese Type II diabetic patients. *Diabetologia* 45: 85–96, 2002.
27. **Schulze PC, De Keulenaer GW, Yoshioka J, Kassik KA, Lee RT.** Vitamin D3-upregulated protein-1 (VDUP-1) regulates redox-dependent vascular smooth muscle cell proliferation through interaction with thioredoxin. *Circ Res* 91: 689–695, 2002.
28. **Schulze PC, Yoshioka J, Takahashi T, He Z, King GL, Lee RT.** Hyperglycemia promotes oxidative stress through inhibition of thioredoxin function by thioredoxin-interacting protein. *J Biol Chem* 279: 30369–30374, 2004.
29. **Shalev A, Pise-Masison CA, Radonovich M, Hoffmann SC, Hirshberg B, Brady JN, Harlan DM.** Oligonucleotide microarray analysis of intact human pancreatic islets: identification of glucose-responsive genes and a highly regulated TGFbeta signaling pathway. *Endocrinology* 143: 3695–3698, 2002.
30. **Sheth SS, Castellani LW, Chari S, Wagg C, Thipphavong CK, Bodnar JS, Tontonoz P, Attie AD, Lopaschuk GD, Lusis AJ.** Thioredoxin-interacting protein deficiency disrupts the fasting-feeding metabolic transition. *J Lipid Res* 46: 123–134, 2005.
31. **Turturro F, Friday E, Welbourne T.** Hyperglycemia regulates thioredoxin-ROS activity through induction of thioredoxin-interacting protein (TXNIP) in metastatic breast cancer-derived cells MDA-MB-231 (Abstract). *BMC Cancer* 7: 96, 2007.
32. **Tuttle RL, Gill NS, Pugh W, Lee JP, Koeberlein B, Furth EE, Polonsky KS, Naji A, Birnbaum MJ.** Regulation of pancreatic beta-cell growth and survival by the serine/threonine protein kinase Akt1/PKBalpha. *Nat Med* 7: 1133–1137, 2001.
33. **Wang Y, De Keulenaer GW, Lee RT.** Vitamin D(3)-up-regulated protein-1 is a stress-responsive gene that regulates cardiomyocyte viability through interaction with thioredoxin. *J Biol Chem* 277: 26496–26500, 2002.
34. **Wang Z, Rong YP, Malone MH, Davis MC, Zhong F, Distelhorst CW.** Thioredoxin-interacting protein (txnip) is a glucocorticoid-regulated primary response gene involved in mediating glucocorticoid-induced apoptosis. *Oncogene* 25: 1903–1913, 2006.
35. **Wilson GL, Leiter EH.** Streptozotocin interactions with pancreatic beta cells and the induction of insulin-dependent diabetes. *Curr Top Microbiol Immunol* 156: 27–54, 1990.
36. **Yang Z, Chen M, Fialkow LB, Ellett JD, Wu R, Nadler JL.** The novel anti-inflammatory compound, lisofylline, prevents diabetes in multiple low-dose streptozotocin-treated mice. *Pancreas* 26: e99–e104, 2003.
37. **Yoon KH, Ko SH, Cho JH, Lee JM, Ahn YB, Song KH, Yoo SJ, Kang MI, Cha BY, Lee KW, Son HY, Kang SK, Kim HS, Lee IK, Bonner-Weir S.** Selective beta-cell loss and alpha-cell expansion in patients with type 2 diabetes mellitus in Korea. *J Clin Endocrinol Metab* 88: 2300–2308, 2003.